J Solid State Eletrochem (2004) 8: 390–397
DOI 10.1007/s10008-003-0461-1

ORIGINAL PAPER

M. Grdeń · K. Klimek · A. Czerwiński

A quartz crystal microbalance study on a metallic nickel electrode

Received: 16 May 2003 / Accepted: 19 September 2003 / Published online: 13 November 2003

Abstract Electrochemical processes taking place on a Ni electrode have been investigated with the electrochemical quartz crystal microbalance. At potentials negative of ca. −500 mV vs. SCE, a closed frequency loop is observed without irreversible changes in the mass of the electrode. The phase transition α- $\rightarrow$ β-$Ni(OH)_2$, taking place at potentials positive to −500 mV vs. SCE, is accompanied by an irreversible increase in the mass of the electrode. When $Ni(OH)_2$ is further oxidized, the frequency increase is followed by a decrease, indicating the transport of various species in both directions, i.e. from and into the electrode. During the $Ni(OH)_2$ oxidation reaction the transport of species responsible for the mass increase is slower than the charge transfer process.

Keywords Nickel · Nickel hydroxide · Quartz crystal microbalance

Introduction

Nickel is one of the most common electrode materials. Two of the most important kinds of nickel electrodes investigated so far are metallic nickel electrodes and nickel oxide/hydroxide electrodes. The latter are of special interest owing to their application in alkaline batteries, e.g. Ni-Cd, Ni-Fe and Ni-MH [1, 2].

Contribution to the 3rd Baltic Conference on Electrochemistry, GDAŃSK-SOBIESZEWO, 23–26 APRIL 2003.

Dedicated to the memory of Harry B. Mark, Jr. (February 28, 1934–March 3rd, 2003)

M. Grdeń · K. Klimek · A. Czerwiński (✉)
Department of Chemistry, Warsaw University,
Pasteura 1, 02-093 Warsaw, Poland
E-mail: aczerw@chem.uw.edu.pl

A. Czerwiński
Industrial Chemistry Research Institute,
Rydygiera 8, 01-793 Warsaw, Poland

Nickel hydroxide electrodes, mainly α-$Ni(OH)_2$, are usually obtained by precipitation of $Ni(OH)_2$ from solution [1]. Measurements carried out with the electrochemical quartz crystal microbalance (EQCMB) show that during oxidation of various forms of nickel hydroxides, transport of various species, i.e. water molecules, OH^- ions, protons and alkali metal cations, takes place, depending on the $Ni(OH)_2$ structure and the electrolyte solution composition [3, 4, 5, 6, 7, 8, 9, 10, 11, 12, 13]. The results show that transport proceeds in both directions, i.e. expulsion of one species from the $Ni(OH)_2$ (e.g. protons) is accompanied by intercalation of others (e.g. cations). Moreover, some data suggest that cations could be incorporated as hydrated complexes, together with water molecules [4, 5, 6, 14, 15].

Metallic nickel electrodes are the electrodes prepared from bulk metal samples (foils, wires, powder, etc.) or by electrodeposition of the metal in its reduced form. The analysis of processes taking place on the metallic nickel electrode is usually based on the diagram introduced initially by Bode et al. [16], subsequently verified and modified by other authors [17, 18, 19, 20, 21, 22, 23, 24]. The most common proposed oxidation product at potentials negative of ca. −500 mV vs. SCE is α-$Ni(OH)_2$. Another considered compound is NiO, usually as a minor product [25, 26, 27, 28]. According to the Bode diagram, α-$Ni(OH)_2$, stable at cathodic potentials, is irreversibly transformed into a different crystalline form, β-$Ni(OH)_2$, at potentials positive to ca. −500 mV vs. SCE. The latter compound could be generated in more than one layer [29, 30, 31]. Oxidation of $Ni(OH)_2$ at potentials positive to ca. 400 mV vs. SCE leads to generation of compounds of nickel with higher valence states. There are still doubts concerning both the structure and the stoichiometry of the compounds. The most commonly proposed structures are β-NiOOH and γ-NiOOH, which differ in structure [18, 22, 32]. Among other products proposed are NiO_2 and Ni_2O_3 [21, 32, 33]. Another process which is still not fully explained is hydrogen adsorption/absorption in/on a nickel

electrode. The oxidation currents of both forms of hydrogen probably overlap the currents observed due to the generation of $Ni(OH)_2$ [17, 29, 34, 35]. It is very difficult to distinguish these processes.

Various kinds of techniques have been used for investigation of the electrochemical processes on Ni electrodes in basic solutions, including AC impedance spectroscopy [36, 37, 38], AFM [39], IR [20], Raman [40], UV-VIS [17, 31] and ellipsometric [27, 41, 42] spectroscopies. Although there are many EQCMB studies on nickel hydroxides [3, 4, 5, 6, 7, 8, 9, 10, 11, 12, 13, 43], there are no published results with EQCMB experiments carried out on metallic nickel electrodes.

In this paper, we present the results of an EQCMB investigation on a metallic nickel electrode in basic solution when the electrode potential is cycled in a limited potential range. The results are compared with known data concerning $Ni(OH)_2$ electrodes [3, 4, 5, 6, 7, 8, 9, 10, 11, 12, 13, 43] and with the data obtained in our previous study on Pd-Ni alloys [44].

Experimental

Nickel was electrodeposited at a constant potential (−1000 mV vs. SCE) from a bath containing $NiSO_4$, Na_2SO_4 and H_3BO_3, as described previously [34]. All solutions were prepared using Millipore water and analytical grade reagents. The solutions were deaerated with an argon stream. All measurements were carried out at room temperature. All potentials are referred to the SCE electrode.

The EQCMB (type 224) was the same as that used in our previous work [45, 46]. The construction has been described in detail by Kutner and co-workers [47]. 5 MHz AT-cut gold-coated crystals with a diameter of 14 mm (ITR, Poland) were used. The EQCMB was coupled with a potentiostat (Elpan EP20A) and a linear sweep generator (Elpan EG20). Frequency measurements were carried out with a universal counter (HP 53131A). Both the galvanostat/potentiostat and the frequency counter were coupled with a PC computer via an ACD/ADC converter. The EQCMB was calibrated in acidic $AgClO_4$ solution in the same way as in our previous work [45, 46]. The obtained mass sensitivity was 10.8 ng Hz^{-1}.

The most desired form of presentation of the EQCMB results is a value of the mass per mole unit. It can be obtained by dividing the mass change (Δm) by the charge passed during the process, q: $M_a \approx \Delta f/q$. The q value can then be converted into the number of moles of electroactive species when the number of electrons exchanged by one electroactive species is known. Owing to the fact that processes different from pure mass changes of species directly involved in charge transfer process also influence the measured frequency changes obtained, the M_a value will be further called the "apparent molar mass", as used in our earlier work [44, 46].

Results and discussion

General voltammetric and gravimetric behavior of the metallic Ni electrode

Figure 1 presents CV and gravimetric curves recorded for a Ni electrode in 0.1 M KOH solution in the potential range from −1000 to 600 mV. Three potential regions, (a), (b) and (c), clearly indicated in the figure, correspond to:

(a) Below ca. −500 mV: oxidation of metallic nickel, probably to α-$Ni(OH)_2$. Other processes that are also considered in this potential range are hydrogen adsorption/absorption and subsequent desorption [17, 29, 34, 35, 37].
(b) From ca. −500 mV to ca. 400 mV: further oxidation of nickel, including a α- $\rightarrow$ β-$Ni(OH)_2$ phase transition.
(c) Above 400 mV: oxidation of Ni(II) to higher valence states; most commonly proposed compounds are various forms of NiOOH.

When the electrode potential is continuously scanned below −500 mV on a stabilized gravimetric curve (after a

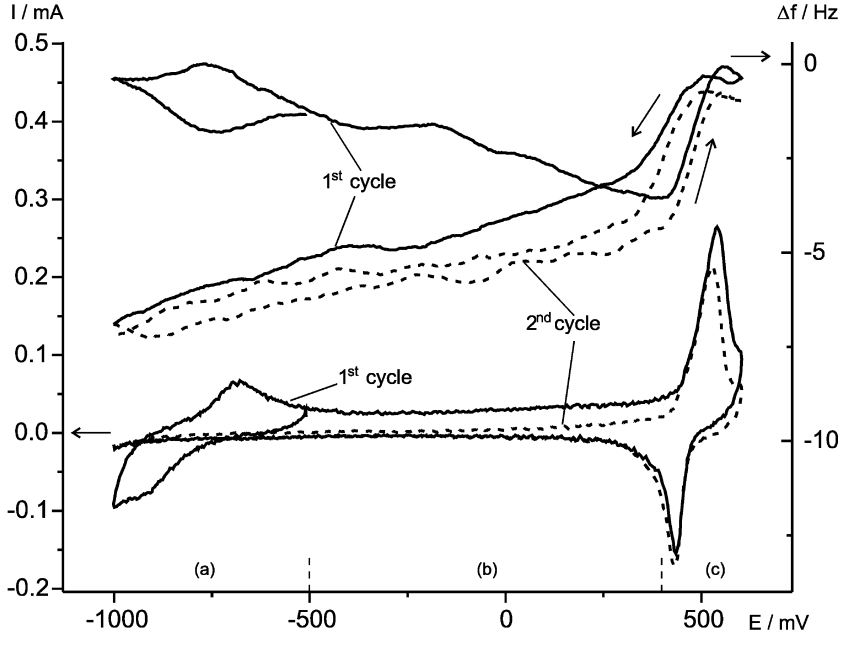

Fig. 1 Voltammetric (*lower*) and gravimetric curves (*upper*) for a metallic Ni electrode in the potential range −100 to 600 mV. *Continuous line*: first cycle; *dashed line*: second cycle; 0.1 M KOH solution, 20 mV s^{-1}. The letters (*a*), (*b*) and (*c*) denote characteristic potential regions described in the text

few tens of cycles), a closed frequency loop is observed without any irreversible mass gain or loss. There is no indication of irreversible nickel dissolution according to previous reports on low Ni dissolution in basic solutions [25, 48]. Thus, the processes taking place in this potential region can be considered reversible.

The anodic peak observed at ca. −700 mV is accompanied mainly by a mass increase, indicating that the process of electrode oxidation (mass increase), probably α-$Ni(OH)_2$ generation, is the main reaction responsible for the frequency changes. This observation, however, does not exclude participation of other processes, such as desorption of absorbed/adsorbed hydrogen, which could overlap with the surface oxidation processes also at potentials positive to the reversible hydrogen potential [17, 29, 34, 35, 37]. Some of those processes, i.e. adsorption, are fast enough to influence the results obtained during a fast potential scan. During a negative potential scan the frequency starts to increase as soon as the cathodic current is constituted. Finally, Ni(II) compounds, formed in an anodic scan, are completely reduced in a cathodic potential scan. A detailed investigation of the processes taking place in potential region (a), below −500 mV, is beyond the scope of the present communication and will be reported in a separate paper.

When the positive potential scan limit increases positive to −500 mV, an irreversible frequency decrease is observed (first cycle in Fig. 1). After a subsequent second cycle of electrode polarization with the cathodic vertex potentials at ca. −1000 mV, the gravimetric curve did not return to the previous value. This effect could be interpreted as an irreversible increase of the mass of the electrode due to the α- $\rightarrow$ β-$Ni(OH)_2$ transformation taking place on a Ni electrode in this potential range. This effect is accompanied by the disappearance of the anodic current peak at ca. −700 mV. During the second scan at potentials negative of −500 mV, only a current plateau is observed. This is due to the fact that the electrode surface has been irreversibly covered with a passive layer of nickel hydroxide, most probably β-$Ni(OH)_2$, that could not be reduced back to metallic nickel [17, 18, 19, 21, 26, 28, 35, 48]. The influence of changes in the cathodic vertex potential on processes taking place on an aged Ni electrode will be presented in a separate communication. The electrode subjected to polarization at potentials where the α- $\rightarrow$ β-$Ni(OH)_2$ transition takes place will be called "aged" in further parts of this text.

According to the literature [2, 49], only α-$Ni(OH)_2$ contains incorporated species like water or alkali metal cations, while β-$Ni(OH)_2$ is free from such species. Taking into account these suggestions, one could expect that replacing one layer of α-$Ni(OH)_2$ containing incorporated water and/or cations by one layer of β-$Ni(OH)_2$ free from incorporated species should produce a mass decrease (frequency increase). In contrast, the opposite effect, i.e. a mass increase during the α- $\rightarrow$ β-$Ni(OH)_2$ transformation, observed in Fig. 1, could be explained by the formation of an additional number of β-$Ni(OH)_2$ layers. This is in agreement with the data of other authors [29, 30, 31], who reported that β-$Ni(OH)_2$ forms more than one layer on the surface of a Ni electrode. It is worth noting that the mass increase observed during the first positive potential scan above −500 mV is not monotonous. At potentials ranging from −500 to −200 mV, a frequency plateau is observed. It is likely that water molecules incorporated into the α-$Ni(OH)_2$ film could participate in generation of a β-$Ni(OH)_2$ layer. As a result, the obtained mass gain is smaller than that expected for hydroxide generated with participation of an oxygen-containing species arriving directly from the solution. During the anodic potential scan of an aged Ni electrode in the potential region negative of 400 mV, the frequency increases with potential. The current in this potential region is featureless. Further experiments described in the text were taken over a limited potential region, ca. 600 to 0 mV, the potential range usually used in experiments with $Ni(OH)_2$ electrodes.

In potential region (c), above 400 mV, nickel hydroxides are oxidized to compounds containing nickel ions with a higher valence state, most probably γ- and β-NiOOH [17, 18, 19, 35, 48, 49, 50]. It is known that gravimetric behavior recorded during oxidation of nickel hydroxides is drastically different for α-$Ni(OH)_2$ and β-$Ni(OH)_2$ electrodes. The oxidation of α-$Ni(OH)_2$ induces a general mass increase (frequency decrease), while the oxidation of β-$Ni(OH)_2$ is accompanied by a general mass decrease (frequency increase) [3, 7, 8, 9, 10, 11, 13]. One could expect that similar EQCMB data induced by a α- $\rightarrow$ β-$Ni(OH)_2$ phase transition should be observed also for a metallic Ni electrode. From Fig. 1, however, it is evident that the behavior of the Ni electrode is similar to that observed for the β-$Ni(OH)_2$/β-NiOOH redox couple. Virtually no evidence for the existence of a α-$Ni(OH)_2$/γ-NiOOH redox couple on the Ni electrode is seen. This observation is the same for both KOH and NaOH solutions. We can propose the following explanations of this phenomenon:

1. On a metallic Ni electrode, the α- $\rightarrow$ β-$Ni(OH)_2$ phase transition is completed, i.e. all α-$Ni(OH)_2$ is transformed into β-$Ni(OH)_2$, before the potential region (c) from 400 to 600 mV responsible for $Ni(OH)_2$ oxidation is reached. In the case of nickel hydroxide electrodes, transformation between various forms of $Ni(OH)_2$ and NiOOH was observed in this potential region as a qualitative evolution of a gravimetric profile [3, 8, 9, 11]. The difference between ageing processes on $Ni(OH)_2$ and metallic Ni electrodes could be explained as a result of a difference in the rate of the α- $\rightarrow$ β-$Ni(OH)_2$ phase transition for both kinds of electrodes. For the $Ni(OH)_2$ electrodes, a phase transition is a bulk process which probably needs more time for completion than the time passed during a relatively fast potential scan in region (b) from −500 to 400 mV. In the case of a metallic nickel electrode, however, the

thickness of the generated β-$Ni(OH)_2$ layer is limited to 3–5 layers [17, 18], i.e. much thinner than for $Ni(OH)_2$ electrodes. Thus, on a Ni electrode a nickel hydroxide layer could be thin enough for completing the α- $\rightarrow$ β-$Ni(OH)_2$ phase transformation during a CV scan in potential region (b), from −500 to 400 mV, before potential region (c), positive to 400 mV, is reached. This process is probably not completed for $Ni(OH)_2$ electrodes.

2. The gravimetric behavior of oxygenated nickel compounds generated on metallic Ni electrodes could differ from that reported for nickel hydroxide electrodes. It is know that transport of water molecules and ions plays an important role in the electrogravimetric behavior of $Ni(OH)_2$ electrodes [3, 7, 8, 9, 10, 11, 12]. The incorporation of various species into the crystal lattice of $Ni(OH)_2$ depends on the crystalline structure of the latter. Namely, the more compact the structure, the more difficult the intercalation process. Thus, one could expect that an ion/water intercalation process in $Ni(OH)_2$ generated on the nickel electrode could be impeded due to its structure. In our previous paper [4] it was shown that generation of nickel compounds with a higher valence state on Pd-Ni alloys was accompanied by a strong mass increase. It is known, however, that the lattice constant of these alloys is greater than that of pure nickel [51]. Thus, a more open structure of the alloy could facilitate generation and stabilization of a specific form of nickel hydroxide. As a result, a stable gravimetric profile different than that observed for a metallic nickel electrode was recorded. These observations agree with the data of other authors, who reported differences in the oxidation of $Ni(OH)_2$ generated on metallic nickel and $Ni(OH)_2$ electrodes on the basis of electrochemical and spectrophotochemical measurements [31].

Influence of the electrolyte solution composition

Figure 2 shows frequency–charge plots for anodic scans in the potential range 0–400 mV recorded for an aged Ni electrode in KOH and NaOH solutions. These plots indicate that processes at this potential range are independent of the mass of the cation present in the electrolyte solution. Since both K^+ and Na^+ cations have similar solvation energies and hydration numbers, one can conclude that the abilities of both cations towards adsorption during relatively fast potential scans are similar [52]. This means that cations do not participate in double layer charging nor in faradaic processes observed in this potential range when the potential of the electrode is scanned at 20 mV s^{-1}. The only published results concerning cation adsorption on a Ni electrode in basic solutions show that the adsorbability of alkali metal cations increases with the cation mass increase [53]. Thus, it should be expected that frequency–charge curves recorded in both electrolyte solutions should differ. Taking into account the results presented in Fig. 2, one could conclude that there is no specific adsorption of alkali metal cations at potentials positive to 0 mV.

In the literature there is a lack of data concerning the potential of zero charge (p.z.c.) for a nickel electrode in basic solutions. Since the potential of zero charge of a Ni electrode in basic media is unknown, it is not clear if there is any specific adsorption of K^+ and Na^+ cations at all or if the p.z.c. is located at potentials negative of 0 mV. The lack of influence of the kind of cation on the described processes indicates that water molecules and/or OH^- ions rearrangement or adsorption are responsible for the frequency response in this potential range.

Figure 3 presents stabilized CV and gravimetric curves of an aged Ni electrode in a potential range from 0 to 600 mV. At potential region (c), above 400 mV, one

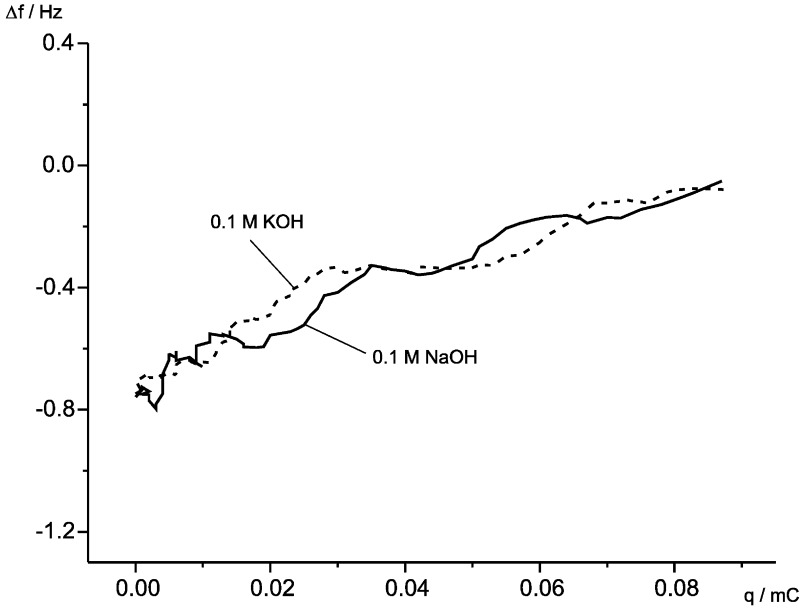

Fig. 2 Frequency vs. charge profile for an aged Ni electrode in various solutions. Anodic scan in the potential range 0–400 mV; 20 mV s^{-1}

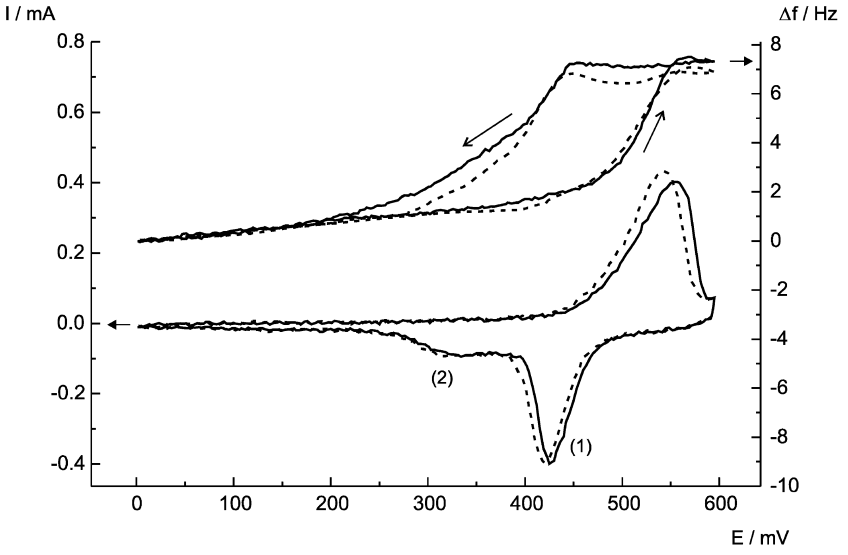

Fig. 3 Cyclic voltammetric (*lower*) and gravimetric curves (*upper*) for an aged metallic Ni electrode in the potential range 0–580 mV in 0.1 M KOH (*dashed line*) and 0.1 M NaOH (*solid line*) solutions; 20 mV s^{-1}. The numbers (*1*) and (*2*) denote current peaks described in the text

anodic and two poorly separated cathodic peaks at (1) ca. 425 mV and (2) ca. 330 mV are observed. The shape of the currents observed on a Ni electrode in this potential range depends on the electrode ageing process as well as on the anodic and cathodic vertex potentials [17, 19, 22, 29, 30, 34, 54]. These currents could be considered as the effect of the overlapping of multiple reactions [22]. During the anodic potential scan, the frequency increase is followed by a small frequency decrease. From the changes in the frequency profile observed in Figs. 1, 3 and 4, it is clear that more than one species participates in the overall $Ni(OH)_2$ oxidation process. One of them is responsible for the initial frequency increase (mass decrease), while the transport of the other causes the subsequent frequency decrease, i.e. the mass increase. Similar shapes of gravimetric curves were interpreted for $Ni(OH)_2$ electrodes as a result of removing certain species (H_2O molecule or proton) from the electrode followed by cation incorporation [6, 14, 15, 43, 55].

This gravimetric response accompanies a relatively wide anodic current peak. During a subsequent cathodic scan a frequency increase is followed by a frequency decrease. The latter part of the gravimetric curve coincides with the beginning of a more anodic peak (1) at ca. 425 mV. Peak (1) is accompanied by a frequency decrease with a greater slope than the wide peak (2) at ca. 330 mV. This suggests that mass transfer during the processes responsible for peak (2) is slower than during the processes generating the currents of peak (1). At the end of peak (2) the frequency–potential curve recorded for cathodic and anodic potential scans overlaps, indicating that the process responsible for mass changes in the potential region of peak (2) is completed. The results presented in Fig. 3 suggest that alkali cation transport accompanies cathodic processes responsible for both cathodic peaks.

Information about the involvement of cations in $Ni(OH)_2$ oxidation processes can be gained from the experiments carried out in KOH and NaOH solutions. The CV and gravimetric curves recorded in 0.1 M KOH and then in 0.1 M NaOH solutions are compared in Fig. 3. At potentials positive to 400 mV, i.e. when $Ni(OH)_2$ is oxidized, both the CV and gravimetric curves are influenced by the kind of cations present in solution. This is observed for both anodic and cathodic potential scans. Since Fig. 2 shows that cations do not influence the double layer charging processes, it is clear that the changes observed in Fig. 3 result from the solution composition and originate from direct participation of cations in a Ni(II) oxidation process. Anodic current peaks are shifted in the potential scale when the solution is changed from NaOH into KOH. In KOH solution, the gravimetric curve accompanying the currents of $Ni(OH)_2$ oxidation is placed at lower frequency values. This concerns both the initial frequency increase as well as the subsequent frequency decrease. It can be seen that the initial frequency increase observed during the anodic potential scan is influenced by the cations. This indicates that cation transport begins before the process of expulsion of species responsible for the frequency increase is completed. It is likely that the subsequent mass increase could be also the result of the incorporation of species other than cations, such as water molecules. An even more dramatic influence of the kind of cation is observed for the cathodic potential scan. The frequency decay in NaOH solution is much slower than in the case of KOH. It is worth noting that although for cathodic peak (1) at ca. 425 mV the frequency–potential slopes are very similar in both electrolyte solutions, a large difference between the gravimetric curves occurs for cathodic peak (2) at ca. 330 mV. Moreover, more than 50% of the overall frequency decrease is connected with peak (2). Peak (2) is wider and less defined than peak (1). This could be the effect of diffusional limitations in the process responsible for these currents. Overall, these experiments suggest that one of the species involved in mass changes during $Ni(OH)_2$ oxidation is an alkali metal cation and

separate electrochemical processes are accompanied by different transport processes.

The difference in the frequency changes recorded during the $Ni(OH)_2$ oxidation process observed for K^+ and Na^+ solutions corresponds to the difference of molar masses for these cations. Kim et al. [9] reported EQCM measurements on $Ni(OH)_2$ deposited on AT- and BT-cut crystals. Those experiments showed that during reactions of the Ni(II)/Ni(III) redox couple, the frequency response is not influenced by stresses generated inside the electrode material. It is not clear if the hydroxide film present on the surface of a metallic Ni electrode behaves in a same manner. However, even if $Ni(OH)_2$ generated on metallic nickel is more compact, which facilitates generation of additional stresses during Ni(II) oxidation, the influence of the kind of cation on the gravimetric plots presented in Fig. 3 indicates that these ions must participate in the overall processes of $Ni(OH)_2$ oxidation. As was proposed for $Ni(OH)_2$ electrodes [4, 5, 6, 10, 14, 15], the cations are incorporated into the bulk of the compound generated during $Ni(OH)_2$ oxidation. In order to avoid the generation of excess positive charge during the incorporation of alkali metal cations, this process is probably accompanied by simultaneous incorporation of OH^- ions [10, 14].

Chronoamperometric results

Figure 4 presents the results of combined voltammetric and potentiostatic experiments. The electrode potential was scanned at a rate of 20 mV s^{-1} and then, at a desired potential value in the $Ni(OH)_2$ oxidation region, E_s, the scan was stopped. After enough time for obtaining a constant frequency value (ca. 60 s), it was then continued again towards a positive potential value (see potential program in the inset in Fig. 4a).

Chronoamperometric (lower) and gravimetric (upper) responses for a Ni electrode recorded as a function of time are presented in Fig. 4b. Although the potential was kept at the E_s value until a constant frequency value was recorded, starting the potential scan in the anodic direction caused a further frequency increase, indicating further progress in the Ni(II) oxidation process. This observation indicates that the process of Ni(II) oxidation is not completed until a high enough potential value is reached. This observation is supported also by results presented in Fig. 4b. The comparison of frequency–time curves recorded for various E_s potential values indicates that for $E_s > 524$ mV the frequency stabilizes at a potential-dependent value, i.e. the greater the E_s value, the lower the stabilized frequency value. Thus, it is likely that the amount of Ni(II) oxidation products is potential dependent.

Figure 4b and Fig. 4c present chronoamperometric and gravimetric responses for a Ni electrode kept at a various E_s values. The current recorded at a constant potential is stabilized within less than 20 s for all potentials in the range 520–580 mV. At potentials positive to ca. 525 mV, a frequency decrease (mass increase) is observed after an initial mass decrease, indicating that transport of another species starts. The comparison of current–time and frequency–time profiles shows that the frequency reaches a constant value after a time longer than that needed for completing the current decay. The time of the frequency decay is not greater than ca. 50 s for all potentials presented in the figure. The fact that both the frequency and the current are stabilized within a relatively short time suggests that the processes under consideration are limited to a few atomic layers below the surface, as was reported by other authors [17]. The difference between the time needed for completing the current and frequency decays indicates that the process responsible for the frequency response observed at potentials positive to ca. 525 mV is much slower than the charge transfer process. This also suggests that the species responsible for frequency decay does not participate directly in the charge transfer process. Current–time and mass–time transient measurements for the oxidation of $Ni(OH)_2$ electrodes show that the transport of counterions, i.e. cations of alkali metals, in the hydroxide layer starts when a sudden change in the slope of the current–time curve is observed [12]. This is probably the result of the formation of the NiOOH phase in the electrode/electrolyte interface. It was suggested that the growth of NiOOH begins at the electrode/substrate interface, while for cation incorporation the presence of NiOOH at the electrode/electrode interface is required [12]. In order to avoid the generation of excess charge and a potential barrier that could stop further oxidation reactions, the rate of transport of the counterions should be similar to the rate of the charge transfer process. In the case of metallic Ni electrodes, however, the frequency decay is still observed even when the current falls to zero (see Fig. 4a). Moreover, taking into account the total charge passed in the one-electron Ni(II) oxidation process, the apparent molar mass calculated for the frequency decay presented in Fig. 4a gives values not greater than 2 g mol^{-1}. Such a small value, as well as the conditions of the electronegativity of the formed film, suggests that transport simultaneously occurs in two directions, i.e. intercalation of one specimen is accompanied by extraction of the other.

Thus, we can conclude that, during the slow frequency decrease observed in Fig. 4a, transport of species responsible for the frequency changes, i.e. alkali metal cations and/or water molecules and OH^- ions, takes place simultaneously in both directions. The apparent molar mass calculated for the one-electron oxidation process for the initial frequency increase during the anodic potential scan in region (c), above 400 mV, strongly exceeds 1 g mol^{-1}, the value expected for expulsion of a proton from $Ni(OH)_2$. Thus, it is likely that species different from protons, i.e. water molecules or OH^- ions, are removed from the electrode during $Ni(OH)_2$ oxidation. Generally, taking into account the observation presented in the above text that more than

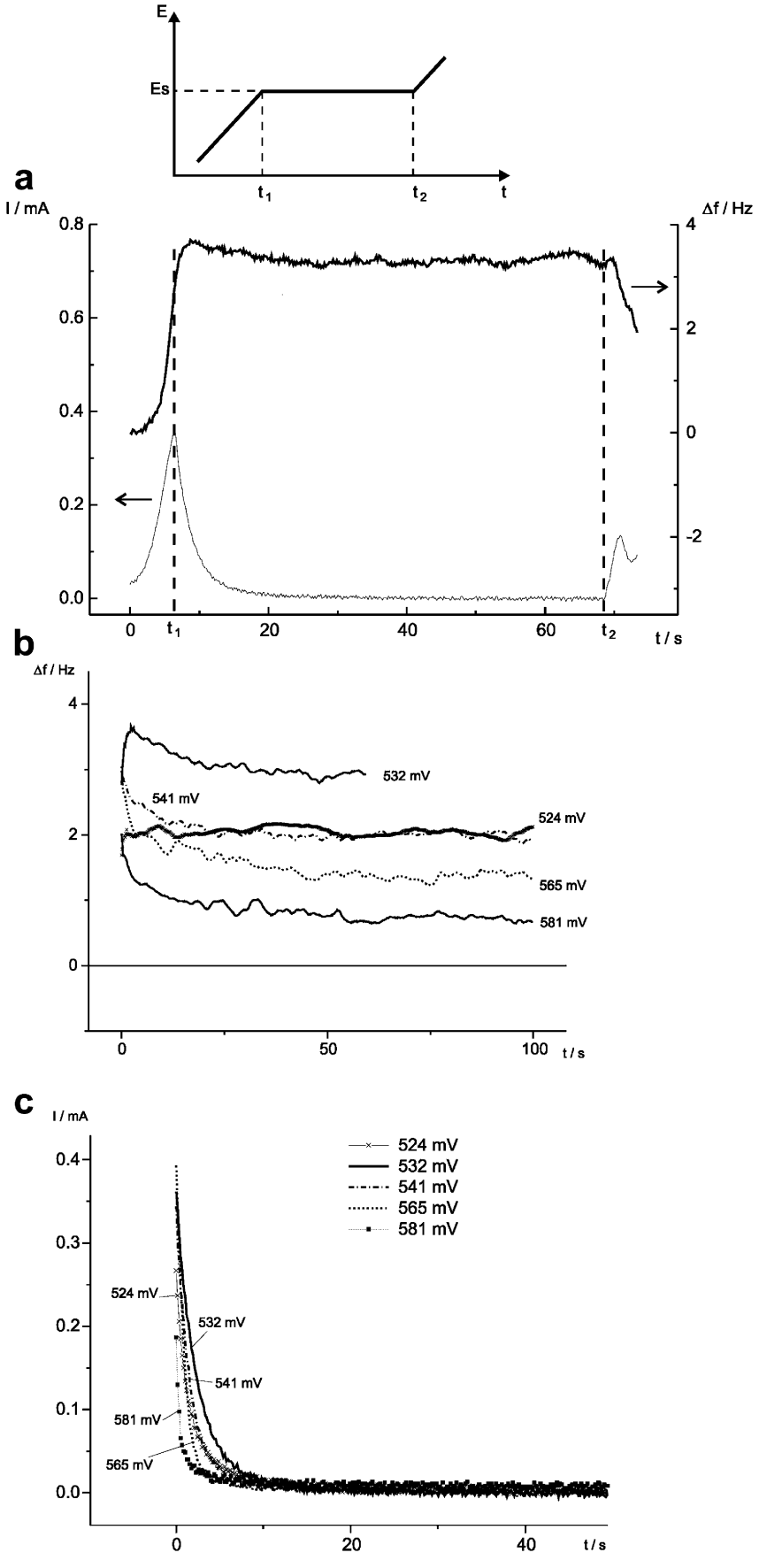

Fig. 4 a Current–time (*lower*) and frequency–time (*upper*) profiles for an aged metallic Ni electrode in 0.1 M NaOH solution. Potential program applied to the electrode presented in the inset. **b** Frequency vs. time profiles recorded for various potential values; 0 denotes the frequency level just before the start of the Ni(II) oxidation process; E_s are potential values indicated on the plot. **c** Similar to **b** but current vs. time plots. Potential scan rate 20 mV s^{-1}

one species participate in the mass exchange during $Ni(OH)_2$ oxidation, it is clear that any calculations of "apparent molar mass" are doubtful since the effective mass transport results in at least two simultaneous transport processes. The EQCM results give us information about the transport processes taking place during oxidation of $Ni(OH)_2$ and subsequent reduction of the products.

Conclusions

The irreversible transformation of nickel hydroxides at potentials positive to ca. −500 mV is accompanied by the irreversible increase in the mass of the electrode.

The gravimetric profile for oxidation of nickel(II) compounds on a metallic Ni electrode is close to that observed for β-$Ni(OH)_2$ electrodes. This profile is already recorded during the first scan in this potential range.

The oxidation of Ni(II) is accompanied by a mass decrease, which is followed by a mass increase. This process depends on the kind of cation present in solution, indicating that K^+ and Na^+ ions are incorporated into the generated film, probably as counterions.

During Ni(II) oxidation, transport of species responsible for the mass changes is slower then the charge transfer process.

The amount of nickel oxides with valence states higher than II depends on the electrode potential.

The processes taking place on the aged Ni electrode in the potential range 0–400 mV are independent of the kind of cation present in the electrolyte solution.

Acknowledgements This work was financially supported by the Department of Chemistry, Warsaw University, grant no. 120-501/68-BW-1562/03/2002.

References

1. Desilvestro J, Haas O (1990) J Electrochem Soc 137:5C
2. McBreen J (1990) The nickel oxide electrode. In: White RE, Bockris JO'M, Conway BE (eds) Modern aspects of electrochemistry, vol. 21. Plenum, New York, pp 29–63
3. Kim MS, Kim KB (1998) J Electrochem Soc 145:507
4. Cordoba-Torresi SI, Gabrielli C, Hugot-Le Goff A, Torresi R (1991) J Electrochem Soc 138:1548
5. Bernard P, Gabrielli C, Keddam M, Takenouti H, Leonardi J, Blanchard P (1991) Electrochim Acta 36:743
6. Faria IC, Torresi R, Gorenstein A (1993) Electrochim Acta 38:2765
7. Gonsalves M, Hillman AR (1998) J Electroanal Chem 454:183
8. French HM, Henderson MJ, Hillman AR, Veil E (2001) J Electroanal Chem 500:192
9. Kim MS, Hwang TS, Kim KB (1997) J Electrochem Soc 144:1537
10. Cheek GT, O'Grady WE (1997) J Electroanal Chem 421:173
11. Mo Y, Hwang E, Scherson DA (1996) J Electrochem Soc 143:37
12. Pyun SI, Kim KH, Han JN (2000) J Power Sources 91:92
13. Ohligschläger T, Schwitzgebel G (2001) Phys Chem Chem Phys 3:5290
14. Carbonio RE, Macagno VA, Arvia AJ (1984) J Electroanal Chem 177:217
15. Corrigan DA, Knight SL (1989) J Electrochem Soc 136:613
16. Bode H, Dehmelt K, Witte J (1966) Electrochim Acta 11:1079
17. Hahn F, Beden B, Croissant MJ, Lamy C (1986) Electrochim Acta 31:335
18. Beden B, Floner D, Leger JM, Lamy C (1985) Surf Sci 162:822
19. Schrebler-Guzman RS, Vilche JR, Arvia AJ (1978) J Electrochem Soc 125:1578
20. Beden B, Bewick A (1988) Electrochim Acta 33:1695
21. Desilvestro J, Corrigan DA, Weaver MJ (1988) J Electrochem Soc 135:885
22. Schrebler Guzmn RS, Vilche JR, Arvia AJ (1979) J Appl Electrochem 9:321
23. Sac-Epée N, Palacn MR, Beaudoin B, Delahaye-Vidal A, Jamin T, Chabre Y, Tarascon JM (1997) J Electrochem Soc 144:3896
24. Wen TC, Hu CC, Li YJ (1993) J Electrochem Soc 140:2554
25. Simpraga R, Conway BE (1990) J Electroanal Chem 280:341
26. Melendres CA, Pankuch M (1992) J Electroanal Chem 333:103
27. Paik W, Szklarska-Śmiatowska Z (1980) Surf Sci 96:401
28. Hu CC, Wen TC (1998) Electrochim Acta 43:1747
29. Jaksic MM, Brun J, Johansen B, Tunold R (1995) Int J Hydrogen Energy 20:265
30. Visintin A, Chialvo AC, Triaca WE, Arvia AJ (1987) J Electroanal Chem 225:227
31. Zhang C, Park SM (1989) J Electrochem Soc 136:3333
32. Oblonsky LJ, Devine TM (1995) J Electrochem Soc 142:3677
33. Melendres CA, Xu S (1984) J Electrochem Soc 131:2239
34. Dmochowska M, Czerwiński A (1998) J Solid State Electrochem 2:16
35. Vissher W, Barendrecht E (1980) J Appl Electrochem 10:269
36. Żółtowski P (1993) Electrochim Acta 38:2129
37. Chun JH, Ra KH, Kim NY (2002) J Electrochem Soc 149:E325
38. Madou MJ, McKubre MCH (1983) J Electrochem Soc 130:1056
39. Kowal A, Niewiara R, Peronczyk B, Haber J (1996) Langmuir 12:2332
40. Melendres CA, Paden W, Tani B, Walczak W (1987) J Electrochem Soc 134:762
41. Wronkowska AA (1989) Surf Sci 214:507
42. de Souza LMM, Kong FP, McLarmont FR, Muller RH (1997) Electrochim Acta 42:1253
43. Rosolen JM, Decker F, Fracastro-Decker M, Gorenstein A, Torresi RM, Cordoba de Torresi SI (1993) J Electroanal Chem 354:273
44. Grdeń M, Kuśmierczyk K, Czerwiński A (2002) J Solid State Electrochem 7:43
45. Grdeń M, Kotowski J, Czerwiński A (1999) J Solid State Electrochem 3:348
46. Grdeń M, Kotowski J, Czerwiński A (2000) J Solid State Electrochem 4:273
47. Koh W, Kutner W, Jones MT, Kadish KM (1993) Electroanalysis 5:209
48. Hopper MA, Ord JL (1973) J Electrochem Soc 120:183
49. Singh D (1998) J Electrochem Soc 145:116
50. Fleischmann M, Oliver A, Robinson J (1986) Electrochim Acta 31:899
51. Sakamoto Y, Yuwasa K, Hirayama K (1982) J Less-Common Met 88:115
52. Bockris JO'M, Reddy AKN (1998) Modern electrochemistry: ionics. Plenum, New York, pp 101–110
53. Kudriavceva ZI, Openkin VA, Zhuchkova NA, Khrushcheva EI, Shutilova NA (1975) Elektrokhimiya 11:1488
54. Seghiouer A, Chevalet J, Barhoun A, Lantelme F (1998) J Electroanal Chem 442:113
55. Passerini S, Scrosati B (1994) J Electrochem Soc 141:889